· Article ·
doi: 10.13679/j.advps.2014.3.00133

Advances in Polar Science
September 2014 Vol. 25 No. 3: 133-137

Mirror seeing of the Antarctic survey telescope

ZHANG Kaiyuan[1,2]*, LI Zhengyang[1,2], YUAN Xiangyan[1,2,3] & PEI Chong[1,2]

[1] Nanjing Institute of Astronomical Optical & Technology, National Astronomical Observatories, CAS, Nanjing 210042, China;

[2] University of Chinese Academy of Sciences, Beijing 100049, China;

[3] Chinese Center for Antarctic Astronomy, Purple Mountain Observatory, CAS, Nanjing 210008, China

Received 17 February 2014; accepted 8 July 2014

Abstract Site testing results indicate that Antarctic Dome A is an excellent ground-based astronomical site suitable for observations ranging from visible to infrared wavelengths. However, the harsh environment in Antarctica, especially the very low temperature and atmospheric pressure, always produces frost on the telescopes' mirrors, which are exposed to the air. Since the Dome A site is still unattended, the Antarctic telescope tubes are always designed to be filled with dry nitrogen, and the outer surfaces of the optical system are heated by an indium-tin oxide thin film. These precautions can prevent the optical surfaces from frosting over, but they degrade the image quality by introducing additional mirror seeing. Based on testing observations of the second Antarctic Survey Telescope (AST3-2) in the Mohe site in China, mirror seeing resulting from the heated aspheric plate has been measured using micro-thermal sensors. Results comparing the real-time atmospheric seeing monitored by the Differential Image Motion Monitor and real-time examinations of image quality agree well.

Keywords **mirror seeing, Antarctic survey telescopes, Dome A, turbulence**

Citation: Zhang K Y, Li Z Y, Yuan X Y, et al. Mirror seeing of the Antarctic survey telescope. Adv Polar Sci, 2014, 25: 133-137, doi: 10.13679/j.advps.2014.3.00133

1 Introduction

Preliminary site testing carried out since the beginning of 2008 reveals that Antarctic Dome A is very likely to be the best astronomical site on Earth, even better than Dome C, and is suitable for observations ranging from visible to infrared and sub-millimeter wavelengths. The excellent atmospheric seeing makes Dome A capable of high-resolution imaging. After the Chinese Small Telescope Array[1] and the first Antarctic Survey Telescopes (AST3-1)[2] were mounted on Dome A, the other two Antarctic Survey Telescopes were developed. The harsh environment at Dome A, especially the very low temperature and half atmospheric pressure, always frosts the telescopes mirrors, which are exposed to the air. In the worst cases, the transmittance of the telescope is too low for observations because of the blurred optical surfaces. To solve this problem, the tube of AST3-2 is sealed and filled with dry nitrogen to stop the in-tube optical surfaces frosting over. Moreover, the outer surface of the aspheric plate was coated with an indium-tin oxide (ITO) thin film, which can be heated to be a little warmer than the ambient air to avoid the frosting problem. The temperature difference between the heated surface and the ambient air must be low to decrease the influence of mirror seeing on image quality. A 2℃ temperature difference for AST3-2 was achieved while the power consumption of the ITO coating was only about 8 watts.

In November 2013, AST3-2 was mounted for testing observations on the Mohe site (53°28′23″N, 122°22′11″E), which is the coldest and northernmost part of China with winter temperatures ranging from about –20℃ to –50℃ . Frost and ice crystals easily build up on the outer surface of the optical system, which is similar to what happens on Antarctic

* Correspond author (email: kyzhang@niaot.cas.cn)

Dome A. Excluding the tracking accuracy, the real-time image quality of the telescope is determined by the optical design and alignment, local atmospheric seeing[3], mirror seeing, the tube seeing and the non-uniformity of the refractive index of the heated optical surface. In this study, we mainly conclude that the mirror seeing is due to the warmer aspheric plate. The measurement of mirror seeing introduced by the heated mirror was accomplished using micro-thermal sensors, and the preliminary data are published in the paper, as well as the atmospheric seeing data monitored by the Differential Image Motion Monitor (DIMM), which was mounted on AST3-2.

2 Theory of the mirror seeing measurement

In general, the convection that results from a heated mirror can develop into weak but effective turbulence. The turbulence layer above the entrance pupil will cause a reduction in the image quality, noted as an increase in the seeing full width at half maximum (FWHM).

In the inertial domain of the turbulence, which is between the outer scale L and the inner scale l, Tatarskii[4] found that the temperature structure function is as follows:

$$D_T(\Delta r) =< (T(r) - T(r+\Delta r))^2 > \qquad (1)$$

and agrees with the 2/3 power law, as shown in Eq. (2):

$$D_T(\Delta r) = C_T^2(\Delta r)^{2/3} \qquad (l < r < L)\,. \qquad (2)$$

C_T^2 is the temperature structure constant, which indicates the temperature fluctuation intensity in units of $K^2 \cdot m^{-2/3}$. Combining Eqs. (1) and (2), we can obtain the distribution of the temperature constant in the turbulence domain:

$$C_T^2 = \frac{< (T(r) - T(r+\Delta r))^2 >}{(\Delta r)^{2/3}}\,. \qquad (3)$$

The refractive index N of air can be expressed using Cauchy's formula(4):

$$N - 1 = \frac{77.6\times10^{-6}}{T}(1 + 7.52\times10^{-3}\lambda^{-2})\left(P + 4\ 810\frac{\upsilon}{T}\right), \qquad (4)$$

where P is the pressure with the units of mbar, T is the temperature in units of K, λ is the wavelength, and υ is water vapor pressure in mb. The refractive index structure function is[4]:

$$D_N(\Delta r) =< (N(r) - N(r+\Delta r))^2 >= C_N^2(\Delta r)^{2/3}\,. \qquad (5)$$

From the refractive index structure function and Cauchy's formula, the relation between the temperature structure constant C_T^2 and refractive index structure constant C_T^2 can be written as[5]:

$$C_N^2 = C_T^2\left[77.6\times10^{-6}(1 + 7.52\times10^{-3}\lambda^{-2})\frac{P}{T^2}\right]. \qquad (6)$$

In 1965, Fried obtained the Fried parameter r_0 during research on the influence of turbulence on telescopes. The relation between r_0 and the distribution of C_N^2 can be expressed as[6]:

$$r_0 = [0.423k^2\cos(\gamma)^{-1}\int_0^L C_N^2(h)\mathrm{d}h]^{-\frac{3}{5}}, \qquad (7)$$

where λ is the zenith angle of the direction of the observations. The seeing disk is the FWHM of the point spread function, and Dierickk[7] deduced the relation between r_0 and θ_0:

$$\theta_0 = 0.975\ 863\frac{\lambda}{r_0}\,. \qquad (8)$$

From Eqs. (7) and (8), we can obtain the total seeing contribution from different turbulence layers, which can be written as[5]:

$$\theta_{\text{total}} = \left(\sum_{n=1}^{k}\theta_k^{\frac{5}{3}}\right)^{\frac{3}{5}}\,. \qquad (9)$$

3 Measuring the seeing of a heated mirror

At the beginning of the measurement sequence, the temperature of the ambient air was 249.6 K. An 8-watt heater was used to warm the aspheric plate to stop it frosting over. Twelve PT-100 thermal sensors with an accuracy of 0.1 K were assembled in two rows above the aspheric plate, as illustrated in Figure 1c. The real-time temperature fluctuations were recorded by a Yokowaga portable data logger. Meanwhile, the ambient temperature was detected by an extra thermal sensor 5 m away from the telescope; the mean atmospheric pressure was 998.6 mbar.

The 12 sensors were arranged in six pairs, as illustrated by Figure 1d. The parameters of the sensors are listed in Table 1. The first pair was located 1.2 m away from aspheric plate of AST3-2, and the two sensors were separated by 0.1 m. Based on the arrangement of sensors, we were able to measure the temperature fluctuations introduced by the heated mirror.

Eq. (9) implies that the FWHM of each image is due to the accumulation of different turbulence layers. The micro-thermal sensor pairs were used to measure the temperature fluctuation of layers above the heated mirror. At the same time, the atmospheric turbulence was monitored by a DIMM[8] instrument, as shown in Figure 2. The heat introduced by the aspheric mirror may interfere with the accuracy of the DIMM, but we hardly detected any changes in accuracy during our testing work.

4 Results and analysis

The temperature fluctuations above the aspheric plate over 3 successive hours were recorded by the micro-thermal sensors. Over the course of 3 h, the environmental temperature decreased by about 3 K, as shown in Figure 3.

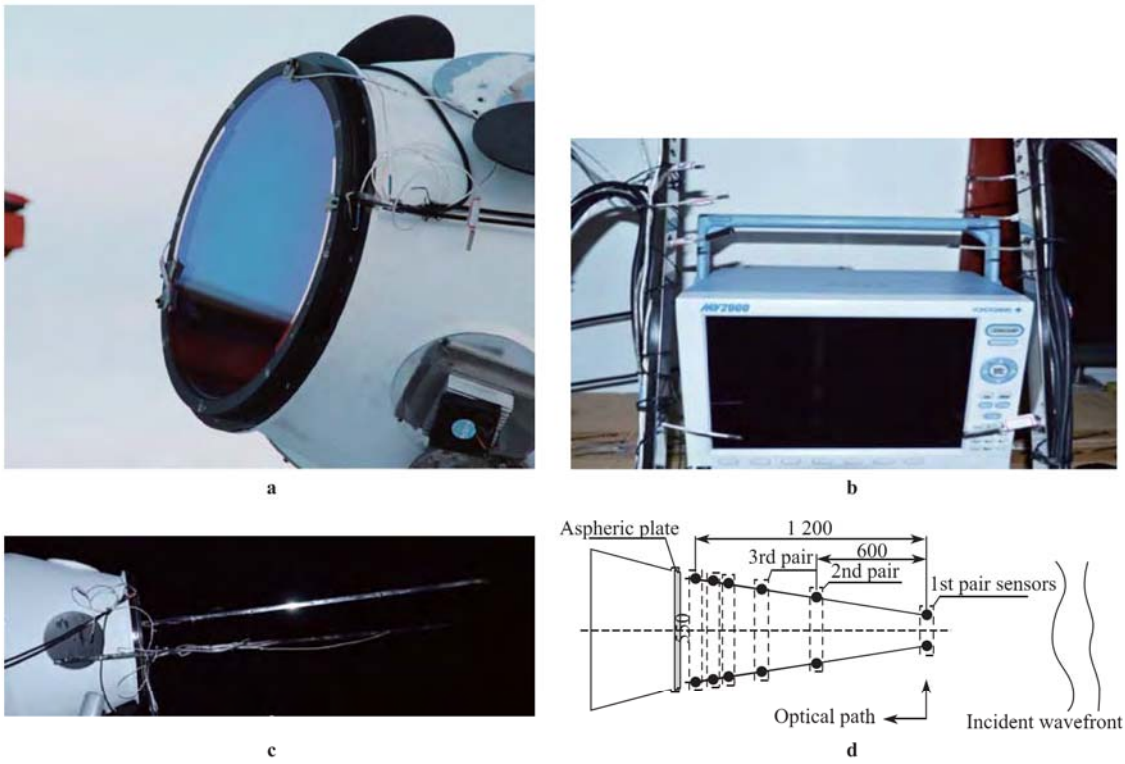

Figure 1 Aspheric plate with ITO coating (**a**); Yokowaga portable data logger (**b**); the installation of micro-thermal sensors on AST3-2 (**c**); schematic plot of the experiment (**d**).

Table 1 The height and distance of each pair of micro-thermal sensors

Number of the micro-thermal sensors	Optical path/m	Distance of the micro-thermal sensor/m
1	0	0.1
2	0.6	0.2
3	0.9	0.3
4	1.1	0.4
5	1.15	0.5
6	1.2	0.55

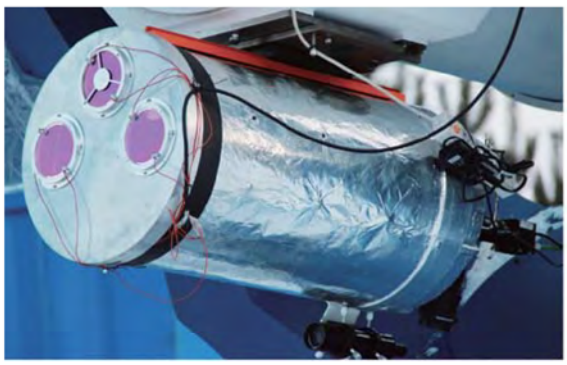

Figure 2 The DIMM instrument.

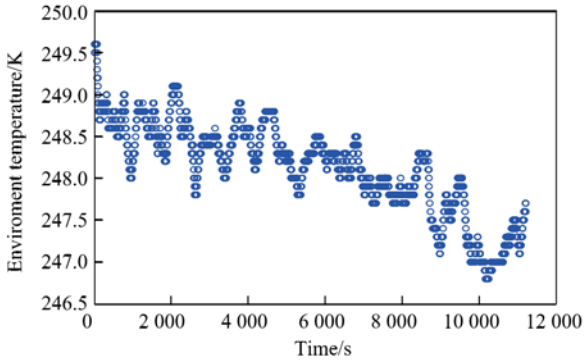

Figure 3 Environmental temperature during the experiment.

The sample frequency of the thermal sensors was 1 Hz. The temperature structure constant C_T^2 was calculated every 321 s using Eq. (3). Figure 4 shows C_T^2 calculated from the first pair of thermal sensors as an example.

The refractive structure constant C_N^2, which quantifies the refractive fluctuation of the inertial domain turbulence, can be deduced from C_T^2 using Eq. (6). Figure 5 shows C_N^2 of the first pair of thermal sensors.

The C_N^2 values of the different layers can be calculated by measuring the temperature fluctuations. The significant Fried parameter r_0 resulting from the mirror seeing can be calculated using Eq. (7). If the r_0 value is smaller than the telescope pupil, the capability of the telescope will be limited by turbulence[9-10]. The entrance pupil of AST3-2 is 0.5 m and

the Fried parameter is 0.21 m. The seeing disk resulting from the turbulence layer above the aspheric plate can be calculated using Eq. (8). The mirror seeing during the test is shown in Figure 6a and the cumulative function of the mirror seeing is shown in Figure 6b.

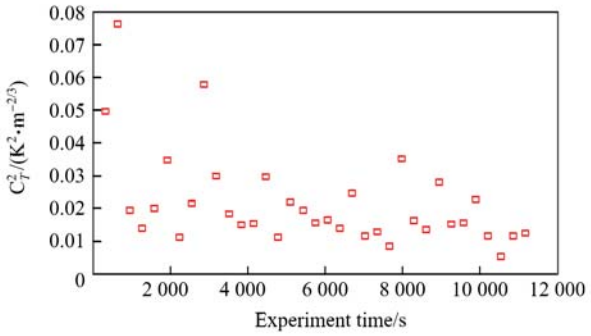

Figure 4 Temperature structure constant coefficient detected by the first pair of thermal sensors.

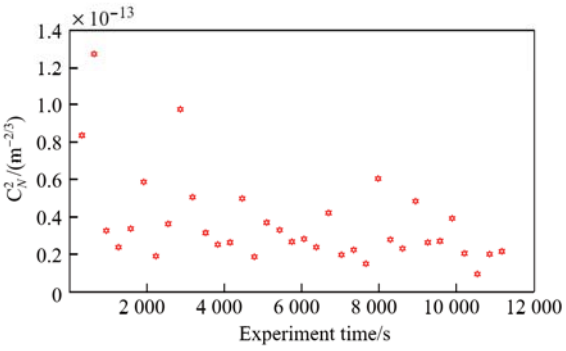

Figure 5 C_T^2 recorded by the first pair of micro-thermal sensors.

The average value of the mirror seeing is 0.508 8″, and a 0.2″ estimated error was included because of the 0.1 K accuracy of the PT100 sensors. In future research, more accurate sensors (0.03 K) will be used to minimize the errors.

During the measurement, a DIMM instrument was assembled to record the atmospheric seeing, which can help us to fully understand the mirror seeing. In the test measurements, the average atmospheric seeing was 2.6″ with a maximum value of 4.2″ and a minimum value of 2.2″, as shown in Figure 7. The FWHM of the star image is about 3.54″, as shown in Figure 8. The data provide a 2.35″ residual angular diameter, which is introduced by the optical quality, tube seeing, the inhomogeneity of the heated mirror and other errors, as shown by Eq. (10):

$$\theta_{\text{other}} = \sqrt{3.54^2 - 2.6^2 - 0.51^2} = 2.35'' . \quad (10)$$

According to the optical design and alignment, the telescope will guarantee an image quality of 1.5″–2.1″ FWHM (full width at half maximum). Hence, the tube seeing or the heated aspheric plate inhomogeneity will induce approximately a 1.0″–1.8″ image degradation, which is the primary contribution to the seeing problem (as opposed to the turbulence introduced by the heated mirror). Because the CCD camera of AST3-2 is placed in the tube and is capable of cooling, the heat generated by the CCD cooling system will induce tube turbulence close to the focal plane. Moreover, the inhomogeneity of the heated aspheric plate results in a non-uniform refractive index, which may be another crucial contribution to the image degradation.

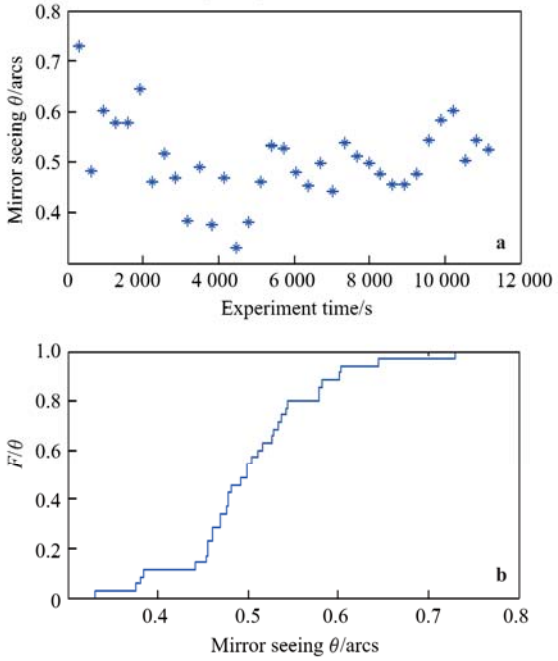

Figure 6 Mirror seeing during the measurement (**a**); the cumulative function of the mirror seeing (**b**).

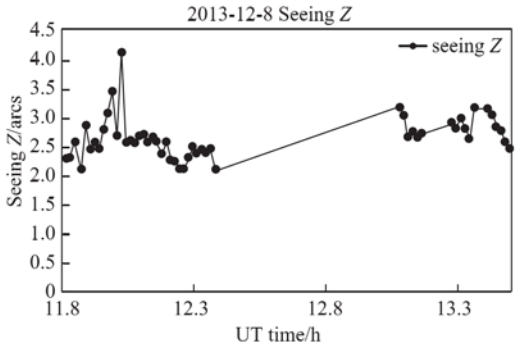

Figure 7 Atmospheric seeing monitored by the DIMM.

5 Conclusions

To check the winterization performance of the Antarctic Survey Telescope, the AST3-2 was mounted on the Mohe site, which is the coldest and northernmost part of China with winter temperatures ranging from about –20℃ to –50℃. Frost and ice crystal can easily build up on the outer surfaces of the optical system, which is similar to what happens on Antarctic Dome A. Keeping the outer optical surfaces warmer than the ambient air using ITO coatings on the aspheric plate of AST3-2 can solve the icing problem. However, the warm

surfaces can lead to mirror seeing, which degrades the image quality. The mirror seeing of the heated aspheric plate was measured using micro-thermal sensors and preliminary data were provided in this paper. Considering the mirror seeing, the local atmospheric seeing measured by an auto DIMM on the AST3-2 tube, the designed image quality, and the estimated tube seeing from the warm CCD between the light path, the real image quality is about 3.5″, which is consistent with the observational results.

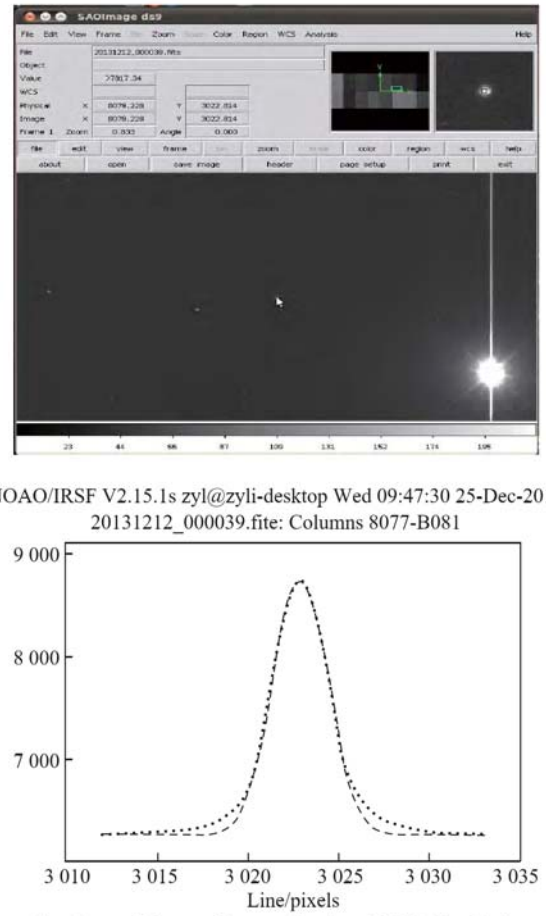

Figure 8 One of the star images by the AST3-2 in Mohe testing observations (FWHM: 3.54″).

Defrosting mirrors and sealed tubes are key features of the Antarctic Telescopes. AST3-2 will be a technical test-bed for the mirror seeing study. AST3-2 will also be very important for the defrosting design and mirror seeing control of the upcoming 2.5-m Kunlun Dark Universe Survey Telescope.

Acknowledgments The authors thank the Chinese Arctic and Antarctic Administration and Polar Research Institute of China and the NSF. This research work was supported by the China Polar Science Strategy Research Fund project (Grant no. 20120314) and the National Natural Science Foundation of China (Grant no. 11190013).

References

1 Yuan X Y, Cui X Q, Liu G R, et al. Chinese Small Telescope ARray (CSTAR) for Antarctic Dome A. Proc. SPIE, 2008, 7012: 70124G,doi:10.1117/12.788748.
2 Li Z Y, Yuan X Y, Cui X Q, et al. Status of the first Antarctic Survey Telescopes for Dome A. Proc. SPIE, 2012, 8444: 84441O, doi: 10.1117/12.925867.
3 Young A T. Seeing: its cause and cure. The Astrophysical Journal, 1974, 189: 587-604.
4 Tatarski V I. Wave propagation in turbulent medium. USA: McGraw-Hill, 1961.
5 Zago L. Engineering handbook for local and dome seeing. Proc. SPIE, 1997, 2871: 726, doi: 10.1117/12.269103.
6 Fried D L. Statistics of a geometric representation of wavefront distortion. JOSA, 1965, 55 (11): 1427-1431.
7 Dierickx P. Optical performance of large ground-based telescope. Journal of Modern Optics, 1992, 39 (3): 569-588.
8 Pei C, Chen H L, Yuan X Y, et al. Development of automated small telescopes as Dome A Site testing DIMM. Proc. SPIE, 2010, 7733: 77334W, doi: 10.1117/12.856762.
9 Fried D L. Limiting resolution looking down through the atmophere. JOSA, 1966, 56 (10): 1380-1384.
10 Fried D L. Optical resolution through a randomly inhomogeneous medium for very long and very short exposure. JOSA, 1996, 56 (10): 1371-1379.